



BOLTON FERDA

PRINCETON UNIVERSITY

24 SEPTEMBER 2015

---

# Retarding Potential Analyzer Theory and Design

---

## Abstract

This paper will focus on the theory and design of Retarding Potential Analyzers (RPAs) which are used to analyze the ion energy distribution of plasma. This paper is written in respect to the RPA designed and built by the author during the summer of 2015 while working in the Electric Propulsion and Plasma Dynamics Lab (EPPDyL) at Princeton University.

## Contents

<b>1</b>	<b>Introduction</b>	<b>2</b>
1.1	Overview . . . . .	2
<b>2</b>	<b>Theory</b>	<b>3</b>
2.1	Debye Length . . . . .	3
2.2	Grid Spacing . . . . .	3
2.3	Mesh Size . . . . .	4
2.4	Measurement . . . . .	4
<b>3</b>	<b>Design</b>	<b>7</b>
3.1	General Constraints . . . . .	7
3.2	Material Selection . . . . .	8
3.2.1	Housing . . . . .	8
3.2.2	Grids . . . . .	9
3.2.3	Detector . . . . .	10
3.2.4	Electrically Insulating Pieces . . . . .	11
3.2.5	Cable . . . . .	13
3.3	Finalized RPA . . . . .	14
<b>4</b>	<b>References</b>	<b>17</b>

# 1 Introduction

## 1.1 Overview

A Retarding Potential Analyzer (RPA) is a plasma diagnostic tool which uses a series of electrostatic grids to selectively repel the constituents of a plasma and a conductor in order to detect the ion energy distribution. Typically, RPAs are constructed using three electrostatically-biased mesh grids with an optional fourth grid. All grids are placed in alignment inside a conductive housing with a conductor placed behind the grids to be used as a detector.

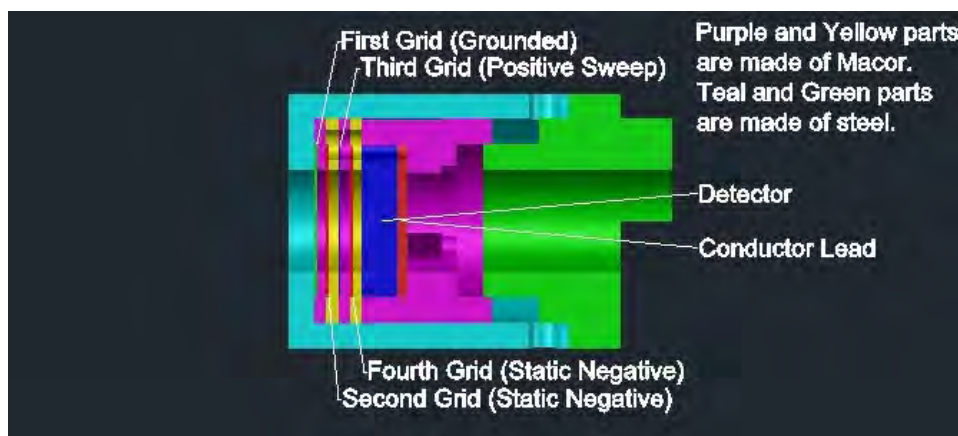


Figure 1: RPA False Color Cross-Section

Each grid plays an important part in the measurement of the energy density. The first grid is held at the floating potential of the plasma or is grounded in order to even out perturbations in the plasma and to prevent the potentials of the other grids from influencing the plasma before it reaches the RPA. The second grid of the RPA is held at a high negative potential. This removes the electrons from the plasma while letting the ions pass through. The third grid of the RPA has a swept voltage applied to it that begins at zero volts and increases to a high positive voltage. This sweep discriminates between the ions of different energies. Initially, at low potentials, all of the ions are let through. However, once the potential becomes high enough, the lower energy ions will be blocked out, resulting in fewer total ions passing through all four grids. The fourth grid of the RPA is considered to be optional. This grid acts as a secondary electron repulsion grid for the electrons that might have been accidentally added to the plasma due to particle bombardment within the RPA. The effects of this grid can sometimes be rather small, but this fourth grid can reduce noise and result in a more accurate reading. [1] Finally, once the ions have passed through

all of the grids, they come into contact with a conductor which is insulated from the housing. The ions then strip electrons from the conductor, creating a current. This current is measured with respect to the voltage of the discriminator grid (third grid).

## 2 Theory

### 2.1 Debye Length

The main parameter of a plasma that determines the configuration of the components in the RPA is the Debye length ( $\lambda_d$ ). The Debye length is the distance at which a particle is significantly influenced by an electrostatic charge. This distance is determined by the temperature ( $T_e$ ) and density ( $n_e$ ) of the electrons in the plasma as can be seen in Equation 1. [2]

$$\lambda_d = \sqrt{\frac{\epsilon_0 k_b / q_e^2}{n_e / T_e + \sum_{ij} z_{ij}^2 / T_i}} \approx \sqrt{\frac{\epsilon_0 k_B T_e}{n_e q_e^2}} \quad (1)$$

The final form of Equation 1 makes the assumption that the ions in the plasma have a much lower mobility than the electrons of the plasma. This means that the ion term will be approximately zero when compared to the electron term making this equation a good approximation.

### 2.2 Grid Spacing

Ideally, the grids are spaced according to Equation 2. This equation is a function of the Debye length ( $\lambda_d$ ), the Voltage difference between two grids ( $V_d$ ), and the electron temperature ( $T_e$ ). [2]

$$x = 1.02 \lambda_d \left( \frac{e V_d}{k_B T_e} \right)^{\frac{3}{4}} \quad (2)$$

Unfortunately, Equation 2 fails to account for an electrostatic phenomenon that can occur in the RPA. If the spacing of the grids is too large, there will be a build-up of charge which will negate the effects of the previous charged grid. For example, if the spacing between the first electron repulsion grid and the discriminator

grid was too large, the build up of positively charged ions behind the electron repulsion grid would cause the positive charge to become large enough to pull electrons through the negatively charged grid. [3]

In order to combat this, the spacing between the grids must be smaller than the approximation given in Equation 2. A common way to do this is to use Equation 3. [3]

$$x \approx 4\lambda_d \quad (3)$$

Equation 3 is definitely simpler than Equation 2, but it is actually just a conservative approximation of Equation 2.

### 2.3 Mesh Size

There are two primary factors in determining the size of the mesh that makes up the grids of the RPA. The first and most important factor is the Debye length. The individual wires in the mesh must be closer together than the Debye length in order to adequately discriminate against the particles of the plasma. If the spacing is too large, particles will pass through the grid due to a dimple of low potential at the center of each cell. However, if the mesh size is too small, the number of particles that can pass through is reduced due to an increase in surface area. Equation 4 shows the largest deviation in the potential field surrounding a grid as a function of wire radius ( $r$ ), grid spacing ( $x$ ), and the length of each cell in the grid ( $a$ ). [4]

$$\frac{\Delta V_r}{V_r} = 1 - \frac{2\pi(x/a) - \ln 4}{2\pi(x/a) - 2\ln(2\sin(\pi r/a))} \quad (4)$$

Balancing the effects of large and small mesh sizes is the second factor in determining the mesh size. For larger mesh sizes, there will be a greater number of particles that will be able to pass through due to a reduction of physical obstacles, creating a larger measurable current on the detector. However, there will also be more particles that will pass through due to the unevenness of the potential field, causing inaccuracies in the measured current. [4]

### 2.4 Measurement

Once the ions pass through the grids of the RPA, they come into contact with the detector, stripping off electrons. The stripping of these electrons creates a measur-

able current of several milliamps. Equation 5 shows the relationship between the energy distribution function ( $f(E)$ ) and the measured current as a function of the discriminator Voltage ( $I_c(V_d)$ ) where the density of the ions ( $n_i$ ), the area of the RPA aperture ( $A_{probe}$ ), and the mass of the ions ( $m_i$ ) are all considered to be constant. [5]

$$I_c(V_d) = -\frac{e^2 n_i A_{probe}}{m_i} \int_{eV_d}^{\infty} f(E) dE \quad (5)$$

By differentiating Equation 5, Equation 6 can be obtained. [5]

$$\frac{dI}{dV} = -\frac{e^2 n_i A_{probe}}{m_i} f(E) \quad (6)$$

As the shape of the distribution function is the most important factor in data analysis and the calculated value using Equation 6 is most likely to be inaccurate due to non-ideal conditions, Equation 7 is used to analyze data. [5]

$$\frac{dI}{dV} \propto -f(E) \quad (7)$$

Figure 2 shows a typical RPA trace with the relationship of Equation 7 imposed on it. The darker, smoother line represents Equation 5. Initially, all of the ions are detected, resulting in a high amperage. However, as the voltage increases, there is a corresponding decrease in the amperage, which indicates that the lower energy ions are being blocked out. Eventually, all of the ions are effectively blocked out, resulting in a zero amperage. [3]

If a higher discriminator voltage or a negative discriminator voltage were applied the readings would not be very useful. This is because the RPA would no longer be taking readings of the plasma, but taking readings of how much it is influencing the plasma. For example, an extremely high positive potential would cause electrons to be pulled away from the detector toward the discriminator. The opposite occurs if a high negative potential is applied.

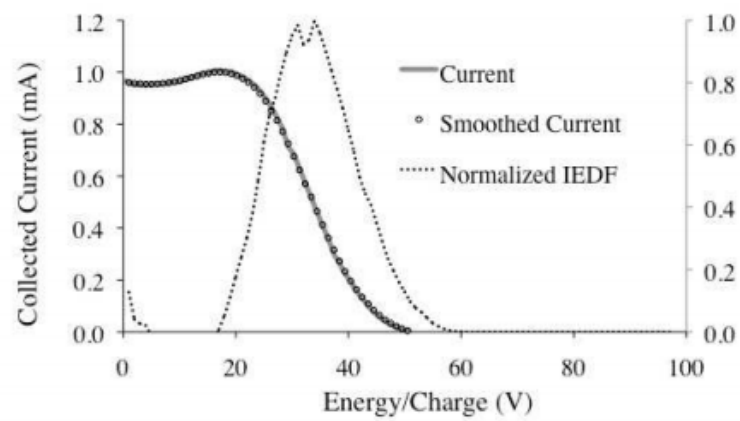


Figure 2: A Typical RPA Trace with the Derived Energy Distribution Imposed



Figure 3: Final Assembled RPA (Penny for Scale)

## 3 Design

### 3.1 General Constraints

When designing and building an RPA, all constraints must be kept in mind. To begin, all of the grids must be chosen and positioned as directed in Section 2. The resulting configuration will be unique as it is dependent upon the anticipated plasma.

Second, the plasma environment in which the RPA will function will most likely have very high temperatures. It is important that all parts are able to withstand the extreme heat of the environment and the possibility of corrosion.

Third, the aperture size must be small when compared to the plasma. If the aperture is too large, the resolution will be poor and important details in the change of the energy distribution over the area of the aperture are lost. Also, if the aperture is too small, too many ions will be blocked out, thus creating a current that is too small to have the desired resolution.

Fourth, all grids and the detector must be electrically insulated from each other and from the housing.



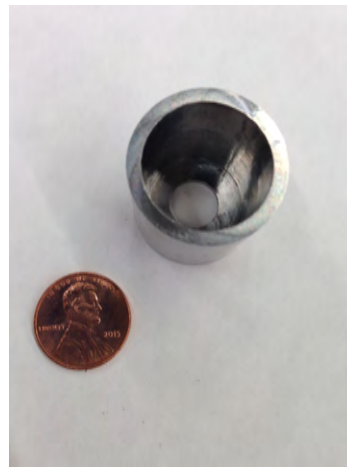
## 3.2 Material Selection

### 3.2.1 Housing

In order to combat the extreme temperatures in which the RPA is expected to operate, the housing was constructed out of 416 marine grade stainless steel. This material was chosen due to its ability to resist heat, corrosion, and regular wear.



(a) Stainless Steel Housing Viewed from Sensing End (Penny for Scale)



(b) Stainless Steel Housing Viewed from Back End (Penny for Scale)



(c) Stainless Steel Housing Cap (Penny for Scale)



(d) Assembled Stainless Steel Housing and Cap

Figure 4

### 3.2.2 Grids

The first, second, and fourth grids were made out of a 304 stainless steel mesh with a cell size of 0.140 mm per side. This size was selected due to the fact that 0.140 mm is much less than the anticipated Debye lengths.

The third grid was made out of 304 stainless steel mesh with a cell size of 0.030 mm per side. This size was selected so that the potential field of the grid would be very uniform and thereby more accurately discriminate between the ions of different energies than the coarser grid.



(a) 0.140 mm Mesh Grid (Penny for Scale)



(b) 0.030 mm Mesh Grid (Penny for Scale)

Figure 5

### 3.2.3 Detector

The detector was made out of pure graphite. This material was chosen due to its high conductivity, high temperature resistance, and low secondary electron emission.



(a) Graphite Detector (Penny for Scale)



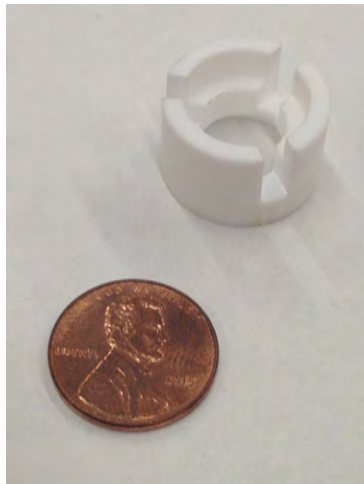
(b) Graphite Detector with Conductor Lead and Macor Housing

Figure 6

### 3.2.4 Electrically Insulating Pieces

All of the insulative pieces were made out of Macor. Macor was chosen due to its machinability and its extremely low conductivity. Two types of pieces were made out of Macor: washers, and the housing. The washers were designed to hold the grids in place, space the grids correctly, and allow wires to pass through to the grids in front of it. The Macor housing also has many functions.

First, it holds the graphite conductor and its stainless steel lead in place. Second, it directs the wires into the appropriate holes in the washers. Third, it compresses the entire assembly together with the help of a spring, which is essential to maintain the correct spacing of the washers and grids.



(a) Macor Housing (Penny for Scale)

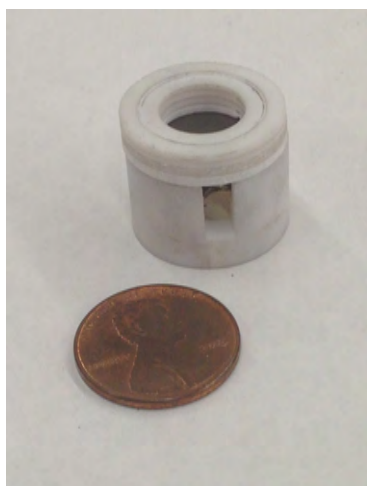


(b) Graphite Detector with Conductor Lead and Macor Housing

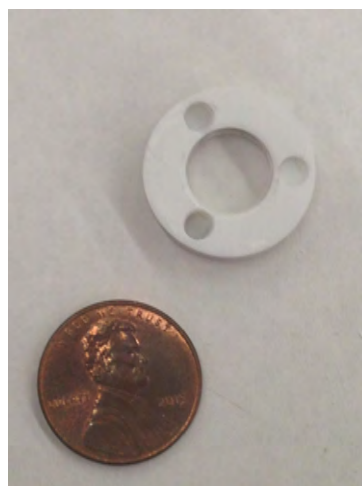
Figure 7



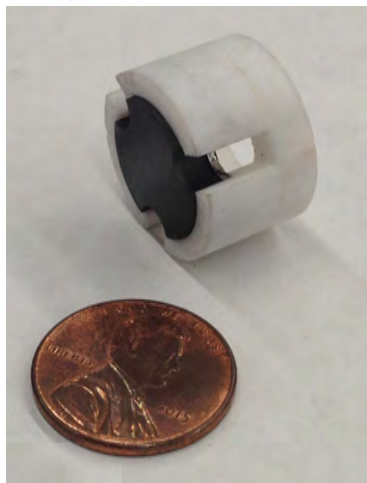
Figure 8: Macor Washer (Penny for Scale)



(a) Graphite Detector Assembled with Macor Housing, Conductor Lead, and Macor Washers (Penny for Scale)



(b) Stacked Macor Washers Showing the Different Depths of the Wire Holes (Penny for Scale)



(c) Graphite Detector Assembled in Macor Housing with Conductor Lead (Penny for Scale)



(d) Assembled Washers, Detector, and Macor Housing to Show Operational Area of RPA (Minus the Grids)

Figure 9

### 3.2.5 Cable

A high temperature, four wire furnace cable was chosen for this RPA. This cable is highly resistant to heat and wear due to its multiple layers of fiberglass and mica insulation.



(a) Fully Assembled RPA Showing the Cable Entering the Back



(b) Cable with Macor Housing

Figure 10

### 3.3 Finalized RPA

Initial results from testing this RPA are extremely promising. It was tested against a RPA from the California Institute of Technology for comparison. Unfortunately, due to time constraints and some required troubleshooting, no accurate data was taken with this RPA. However, it was determined that this RPA shows a very high sensitivity which correlates to a higher resolution and ability to accurately measure the energy distribution of lower-density plasmas compared to the CalTech RPA.

Future testing and use is planned for the RPA at EPPDyL.



Figure 11: Final Assembled RPA

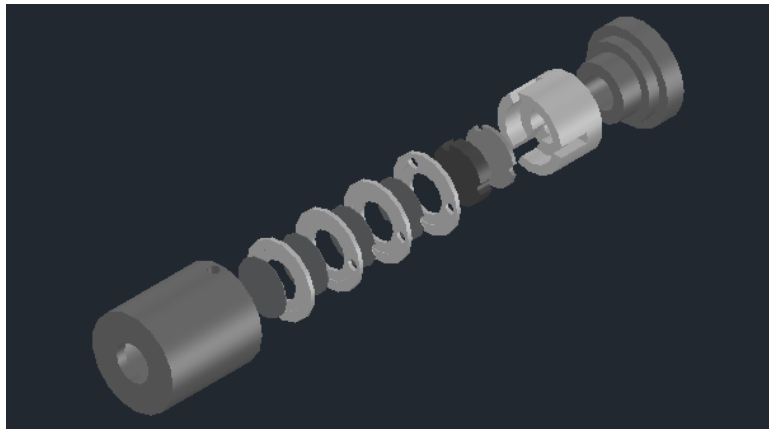


Figure 12: Exploded CAD View of the RPA

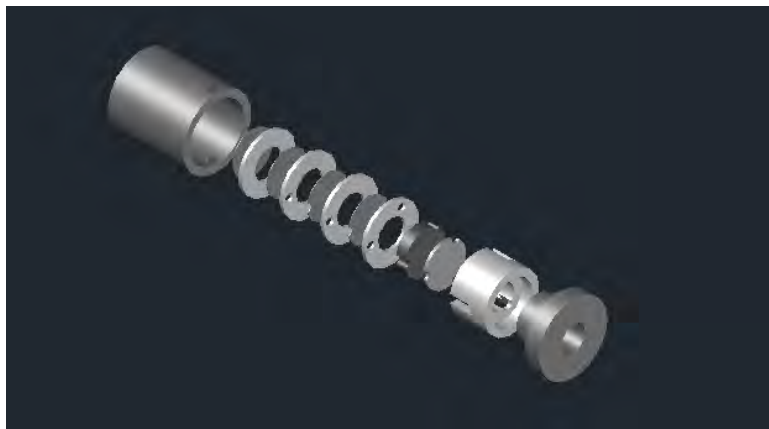


Figure 13: Exploded CAD View of the RPA from the Back



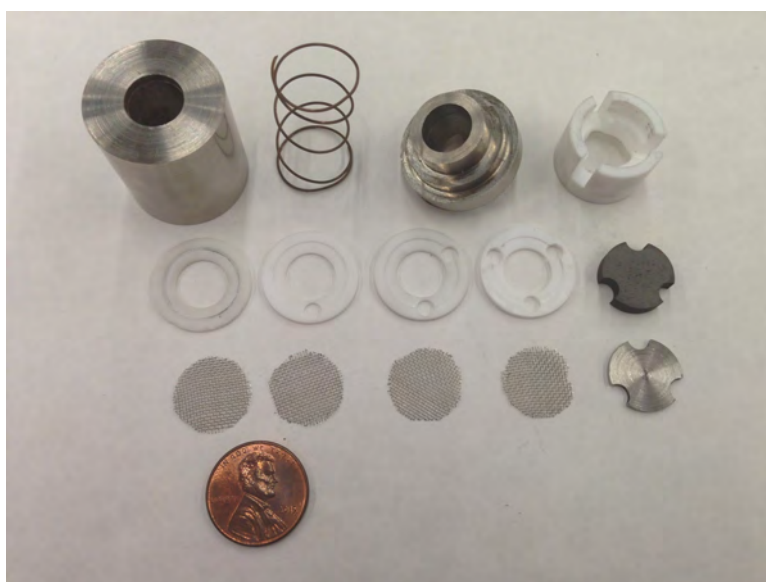


Figure 14: Final Disassembled RPA Showing All Parts (Penny for Scale)

## 4 References

- [1] C. Böhm and J. Perrin, 1993, "Retarding-field analyzer for measurements of ion energy distributions and secondary electron emission coefficients in low-pressure radio frequency discharges," *Review of Scientific Instruments*, 64, pp. 31.
- [2] I. Hutchinson, 2002, *Principles of Plasma Diagnostics*, Second Edition, Cambridge University Press, Cambridge MA.
- [3] K. Lemmer, 2009, "Use of a Helicon Source for Development of a Re-Entry Blackout Amelioration System," Ph. D. Thesis, Aerospace Engineering, University of Michigan.
- [4] C. Enloe and J. Shell, 1992, "Optimizing the energy resolution of planar retarding potential analyzers," *Review of Scientific Instruments*, 63, pp. 1788
- [5] B. Sommers and J. Foster, 2013, "Preliminary Characterization of Ion Energy Spectra Acquired from High Current Hollow Cathodes," *33rd International Electric Propulsion Conference*, 2013